International Journal of GEOMATE, Aug., 2022, Vol.23, Issue 96, pp.40-49
ISSN: 2186-2982 (P), 2186-2990 (O), Japan, DOI: https://doi.org/10.21660/2022.96.3247
Geotechnique, Construction Materials and Environment

FLOW – COMPOSITE HYDRAULIC STRUCTURE – LONGITUDINAL OBSTACLE INTERACTION

*Ihsan Abdulkareem Abdulhussein[1], Rafi Mohammed Qasim[2], Alya Aqeel Mohammed [3] and Qusay Abdulrazzaq Maatooq[4]

[1,2,3,4]Southern Technical University/ Basra Engineering Technical College, Iraq.

*Corresponding Author, Received: 24 Jan. 2022, Revised: 23 May 2022, Accepted: 12 June 2022

ABSTRACT: A composite hydraulic structure can be described as a discharge structure constructed inside a river or an open channel. This experimental study is targeted at investigating the performance of the composite hydraulic structure in consideration of the existence of the longitudinal obstacle in the downstream region of the composite hydraulic structure. This study adopts two different lengths of the longitudinal obstacle. In addition, three different cross-sectional areas of the obstacle in the lateral direction are adopted. Also, the gate of a composite structure has a half-ellipse shape, while the weir of a composite structure has rectangular, triangular, and parabolic shapes, respectively. Seven cases are investigated experimentally. Here, six cases included the longitudinal obstacle, while the last case was without it. The influence of downstream Froude number on the average downstream water depth, downstream flow velocity, upstream Froude number, Reynolds number, and actual discharge is investigated. Also, the relationship between Reynolds number and downstream flow velocity, actual discharge and downstream flow velocity, discharge coefficient and upstream Froude number, discharge coefficient and Reynolds number, discharge coefficient, and actual discharge is investigated, respectively. The results illustrated that the longitudinal obstacle has a moderate influence on the hydraulic characteristics of the composite hydraulic structure regardless of the obstacle length and the obstacle cross-section area. Finally, the hypothesis test is performed to demonstrate the feasibility of the longitudinal obstacle.

Keywords: Gate, Hydraulic structure, Weir, Obstacle, Specific head

1. INTRODUCTION

Flow in rivers, natural channels, artificial channels, and flumes is more sensitive to the presence of obstacles and/or obstacles regardless of the direction of the obstacle and/or obstacles concerning the flow direction. The presence of the obstacle would lead to energy and momentum losses and cause a continuous change in the water level around the obstacle. The problem with the obstacle's presence will grow and develop when a hydraulic structure is built inside the river or channel; it is noticeable that the workability and operation of the hydraulic structure will be influenced by the presence of the obstacle. Generally, the interaction between the hydraulic structure and the obstacle can be considered a big challenge in water resources management and water work. Several researchers deal with the subject of obstacles under the action of fluid motion, regarding the type of fluid and the shape of the obstacle. Qasim et al. [1] experimentally investigated the effect of barriers’ presence on the hydraulic variables that dominate the hydraulic characteristics of the composite hydraulic structure. The experiment examined the influence of barriers’ number, spacing, and, location on the actual discharge quantity, discharge coefficient, and water depth level at the downstream zone. In addition, Qasim et al. [2] conducted experiments with and without an obstruction installed at the downstream region of the composite hydraulic structure. Experiments were performed for two different flow options: the first option concentrates on the free flow while the second concentrates on the submerged flow. Many of the cases that were carried out dealt with different hydraulic variables and dimension variables into the impact of the obstruction on the composite hydraulic structure. Riazi and Jafari [3] performed experimental runs to reveal the influence of the reversed slope on the hydraulic jump on the channel's rectangular section with the rough bed. The result shows an increase in energy dissipation with the increase in slope, while the rough bed decreases the stilling basin length in the submerged hydraulic jump. Samadi- Boroujeni et al. [4] studied the hydraulic jump characteristics over six triangular corrugated beds in a flume that has a rectangular cross-section. Based on their findings, they concluded that the folded bed had an eaffecteddepths. Nabil and Rezak [5] conducted experimental work on the baffle block with the sloping vertical face arranged at the downstream regime of the sluice gate in order ord influence the hydraulic jump length. Hughes and Flack [6] performed experimental runs on the hydraulic jump over a bed of block elements and obtained that the boundary layers could grow faster and the dimensions of the jump would decrease greatly. Mohamed Ali [7] conducted experimental runs on a rough bed adopting cubed elements and obtained a reduction in the length of the hydraulic jump. The present work was not considered previously by the researchers. The main goal of the present study concentrates on the assessment of the hydraulic behavior of composite structures under the action of longitudinal obstacles, which exist in the flume and tdition parallel to the water flow path. This work deals directly with the alteration in the hydraulic characteristics of the composite hydraulic structure under the action of the longitudinal obstacle, which is placed in the downstream zone of the composite hydraulic structure. It is very important to mention this work has not been published previously by any authors. This work also satisfies the confidence level of 99%.

2. RESEARCH SIGNIFICANCE

This paper will be the first step in presenting an experimental study that can describe the interaction between the natural or man-made longitudinal obstacle and the composite hydraulic structure. This is an experimental work to investigate the hydraulic characteristics of the composite hydraulic structure under submerged flow conditions owing to the existence of the longitudinal obstacle. A statistical method is employed to assess the hydraulic results based on a 99% confidence level.

3. FLUID MECHANICS BASICS

The actual discharge which passed through the composite structure can be calculated by adopting the following steps, which are illustrated below. Three different shapes of composite structure are utilized in the experimental study. A non-regular shape was also used for the gate, while a regular shape was used for the weir. Here, we display the steps of the composite actual discharge calculation:

3.1 Triangular weir – Ellipse gate

If the flow state is either free or submerged, the actual discharge that passed through the composite structure can be evaluated according to:

$$Q_{theor} = Q_w + Q_g \tag{1}$$

Theoretical discharge which passed the weir would be evaluated from [9].

$$Q_{weir} = \frac{8}{15}\sqrt{2g}\ \tan\frac{\emptyset}{2}\ \ h^{5/2} \tag{2}$$

Theoretical discharge which passed the gate would be evaluated by utilizing the continuity equation:

The continuity equation as in [8]:

$$Q = VA \tag{3}$$

$$Q_{gate} = V\,A = \sqrt{2gH}\,A \tag{4}$$

$$Q_{act} = c_d\, Q_{theor} \tag{5}$$

$$Q_{act} = c_d\left[\frac{8}{15}\sqrt{2g}\ \tan\frac{\emptyset}{2}\ \ h^{5/2} + \sqrt{2gH}\,A\right] \tag{6}$$

3.2 Rectangular weir – Ellipse gates

If the flow state is either free or submerged, the actual discharge that passed through the composite structure can be evaluated according to:

$$Q_{theor} = Q_w + Q_g \tag{7}$$

Theoretical discharge which passed the weir would be evaluated from [9]:

$$Q_{weir} = \frac{2}{3}\sqrt{2g}\ b\,h^{3/2} \tag{8}$$

Theoretical discharge which passed the gate would be evaluated by utilizing the continuity equation:

The continuity equation as in [8]:

$$Q = VA \tag{9}$$

$$Q_{gate} = V\,A = \sqrt{2gH}\,A \tag{10}$$

$$Q_{act} = c_d\, Q_{theor} \tag{11}$$

$$Q_{act} = c_d\left[\frac{2}{3}\sqrt{2g}\ b\,h^{3/2} + \sqrt{2gH}\,A\right] \tag{12}$$

3.3 Parabolic weir – Ellipse gates

If the flow state is either free or submerged, the actual discharge that passed through the composite structure can be evaluated according to:

$$Q_{theo} = Q_W + Q_g \tag{13}$$

Theoretical discharge which passed the weir would be evaluated from [9]:

$$Q_w = \frac{\pi}{2}\ \sqrt{f\,g}h^2 \tag{14}$$

Theoretical discharge which passed the gate would be evaluated by utilizing the continuity equation:

The continuity equation as in [8]:

$$Q = V A \tag{15}$$

$$Q_g = V\ A = \sqrt{2\ g\ H}\ \ A \tag{16}$$

$$Q_{act} = c_d\ Q_{theo} \tag{17}$$

$$Q_{act} = c_d\ \left[\frac{\pi}{2}\ \sqrt{f\ g}h^2 + \sqrt{2\ g\ H}\ \ A\ \right] \tag{18}$$

For free flow condition

$$H = d + y + h \tag{19}$$

For submerged flow condition

$$H = d + y + h - h_d \tag{20}$$

Where

H: the depth of water upstream, h: water head above weir crest, y: vertical distance between weir and gate, d: gate opening height, A: flow cross-sectional area at the gate, V: flow velocity, f: focal distance, b: Rectangular weir width, θ : Notch angle, g: acceleration due to gravity, Q_w: weir discharge, Q_g: Gate discharge, Q_{theor}: Theoretical discharge , Q_{act}: Actual discharge, c_d: Discharge coefficient.

The Reynolds number as in [10] and Froude number as in [11] were evaluated by using the following equations:

$$R_e = \frac{VL}{\nu} \tag{21}$$

$$F_r = \frac{V}{\sqrt{gy}} \tag{22}$$

Where: ν: the water kinematic viscosity, L: characteristic length which is equivalent to the hydraulic radius (R):

$$R = \frac{A}{P} \tag{23}$$

Where: A is the flow cross-sectional area, while P represents the wetted perimeter.

The specific head (specific energy) of a channel has a rectangular cross-section is evaluated from [12]:

$$E = y + \frac{q^2}{2gy^2} \tag{24}$$

$$q = \frac{Q}{B} \tag{25}$$

Where: q represents the discharge per unit width, Q represents the discharge and B is the width of the channel.

4. EXPERIMENTAL SETUP

Experimental work is carried out by adopting a rectangular flume. The flume has 15cm depth, 7.5cm width and 200cm length. The flume is available in the hydraulic laboratory of Basra Technical Engineering College\ Southern Technical University. In all experiments, the bed of the flume is considered horizontal. Water depth along the length of the flume has been measured by using a points gauge. The volume method was adopted to measure the actual discharge. The composite hydraulic structure and longitudinal obstacle are made by utilizing wood material. 5mm wood sheet thickness is adopted for composite hydraulic structure. The composite hydraulic structure is fixed at a distance of 80cm from the upstream of the flume, while the obstacles are fixed at 30cm and 60cm downstream of the composite hydraulic structure. In each run, when the desired weir head is approached (achieved), the actual discharge, upstream and downstream water depth, is measured, respectively. Figure (1) shows the details of the composite hydraulic structure and figure (2) shows all the considered arrangements of the longitudinal obstacle in the present work. Also, Table (1) shows the dimension of obstacles in the lateral direction. This work comprises 140 experiments.

Table 1. Dimension of the Obstacle

Cases	Cross Section	Length (cm)
1	3cm x 3cm	90
2	3cm x1.5cm	90
3	1.5cm x 1.5cm	90
4	3cm x 3cm	60
5	3cm x1.5cm	60
6	1.5cm x 1.5cm	60

5. RESULTS AND DISCUSSION

The composite hydraulic structure is implied to allow the removal of floating material and sediment material simultaneously. So, it can be considered a symbolic irrigation structure. This structure is devoted to managing the water quantity in the flume, river, and open channel. Figure (3) shows the relationship between the downstream Froude number and the average downstream water depth. The figure reveals remarkable changes. In all cases, when the downstream water depth increases, this leads to a decrease in the Froude number. This will occur owing to the inverse proportionality between Froude number and water depth.

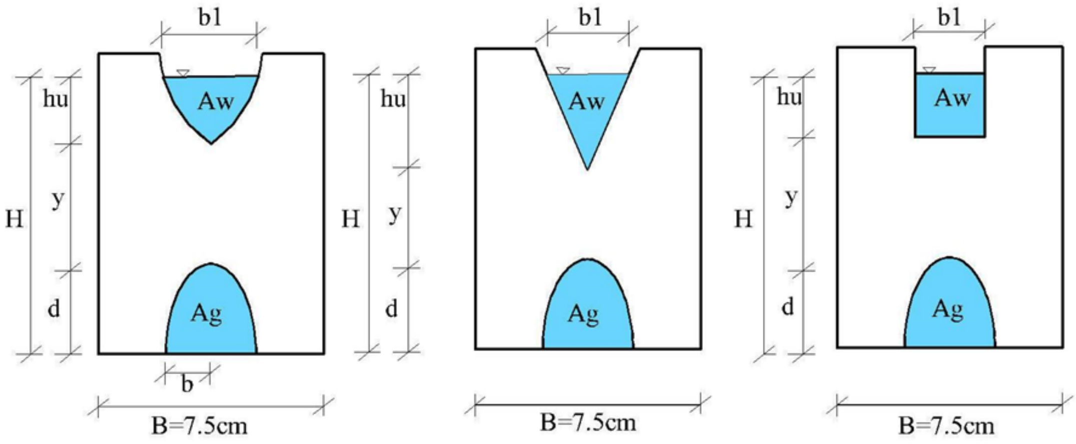

Fig.1 The details of the composite hydraulic structure

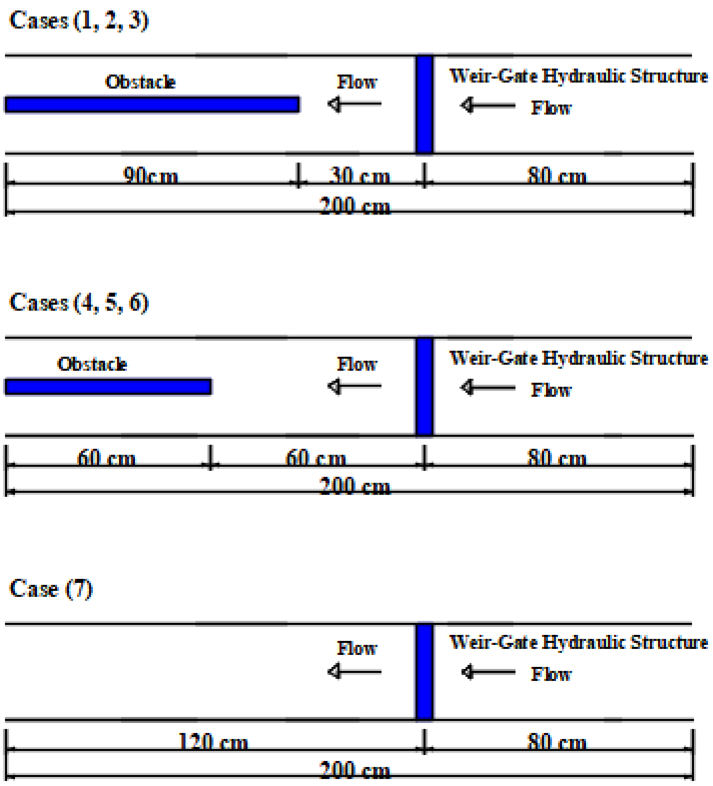

Fig.2 The arrangements of the longitudinal obstacle with the composite hydraulic structure

For case (1), the influence of the obstacle cross-sectional area in the lateral direction and the obstacle length is apparent. Here, the variation in hydraulic response will be attributed to the presence of the obstacle and the interaction between weir flow velocity and gate flow velocity. Figure (4) shows the relation between the downstream Froude number with the flow velocity at the downstream regime. The figure reveals considerable changes. For all cases, the figure illustrates that both the flow velocity and Froude number increase simultaneously without any fluctuation; this occurs due to the direct proportionality between the flow velocity and

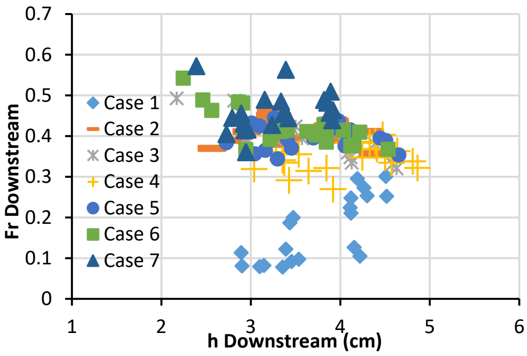

Fig.3 The relationship between downstream Froude Number and downstream water depth

Froude Number. Figure (5) clearly shows the relationship between the downstream Froude number and the upstream Froude number. It is obvious a complex random relationship for all cases except case (1). In case (1) the relation is described as linear. The variation in relationships depends on water depth and flow velocity. These variables control the values of the Froude number. Here, the water depth upstream is higher as compared with downstream. Also, the interference between gate flow velocity and weir flow velocity will reflect on the relationship. Figure (6) clearly shows the relationship between the downstream Froude number and Reynolds number. Both the Froude number and the Reynolds number increase simultaneously because both of them have direct proportionality with the flow velocity. The variation in relationship occurs due to the following: water depth at the stream, the presence of the obstacle an,d the interaction between gate flow velocity and weir flow velocity. It is very important to mention that the water depth has a direct relationship with the Reynolds number and inan verse relationship with th Froude number.

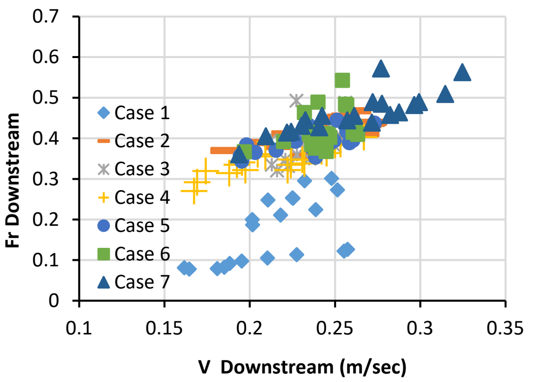

Fig.4 The relationship between downstream Froude number and downstream flow velocity

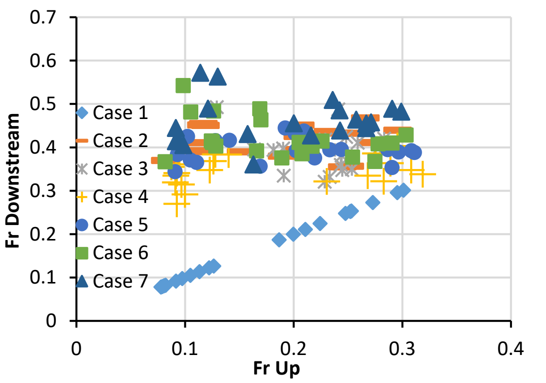

Fig.5 The relationship between downstream and upstream Froude number

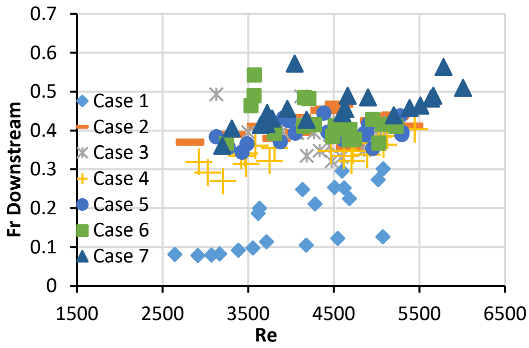

Fig.6 The relationship between downstream Froude number and Reynold's number

Figure (7) illustrates the relationship between the downstream Froude number and$\mathbf{A_g/BH}$. It is clear from the figure that the relation can be described as a non-uniform random relationship. In general, there is no empirical equation or theoretical equation found between $\mathbf{A_g/BH}$ and the downstream Froude number. Here, the Froude number depends on flow velocity adownstreamanand flowepth at dstream while $\mathbf{A_g/BH}$ depends on upstream flow depth and flow velocity at upstream. So the Froude number and the ratio $\mathbf{A_g/BH}$ are considered as independent parameters.

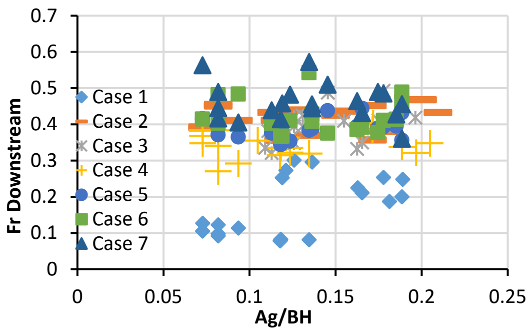

Fig.7 The relation between the downstream Froude number andA_g/BH.

The scatter plot between Reynolds number and flow velocity downstream is plotted in figure (8). It is obvious from the figure (8) that the Reynolds number increases with an increase in flow velocity owing to the direct proportionality between the flow velocity and the Reynolds number. Also, the scatter plot between actual discharge and flow velocity at the same pois int in figure (9). It is obvious frthe om figure (9) that the actual discharge increases with an increase in flow velocity owing to the direct proportionality between the flow velocity and actual discharge according to the continuity equation.

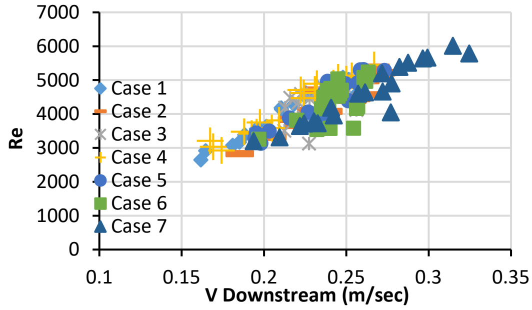

Fig.8 The relation between Reynolds number and downstream Flow velocity

The scatter plot between actual discharge and Froude number at the downstream is plotted in figure (10). Figure (10) shows that the obtained values were distributed randomly for all cases regardless of the longitudinal obstacle presence in the downstream region. There is no direct relationship between actual discharge and the downstream Froude number, whereas both of them depend on flow velocity. Also, both of them have direct proportionality concerning flow velocity. Mainly, the random distribution occurs owing to the interaction between weir flow velocity and gate flow velocity. In addition, the length of the obstacle will affect the flow velocity and this will lead to a reduction in flow velocity.

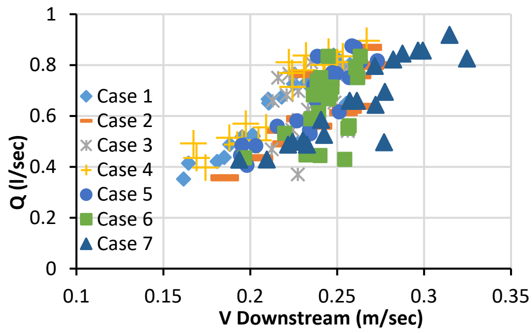

Fig.9 The relation between actual discharge and downstream flow velocity

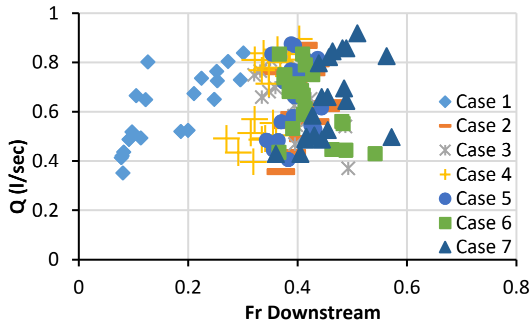

Fig.10 The relation between actual discharge and downstream Froude number

Figures (11) and (12) show the relationship between discharge coefficient with Froude number at upstream and Reynolds number respectively. Both figures illustrate a complex random relationship. Here, it is very necessary to mention that there is no direct relationship between discharge coefficient and Froude number and that there is no direct relationship between discharge coefficient and Reynolds number. All the hydraulic non-dimensional parameters can be considered independent parameters. In addition, all the hydraulic variables which control those parameters are different from one parameter to another. It is very important to infer that the longitudinal obstacle has a minor influence on the relationship shown in figures (11) and (12). However, the random distribution is attributed to the flow velocity and flow depth.

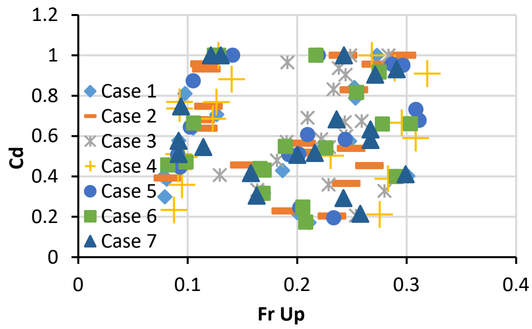

Fig.11 The relation between discharge coefficient and upstream Froude number

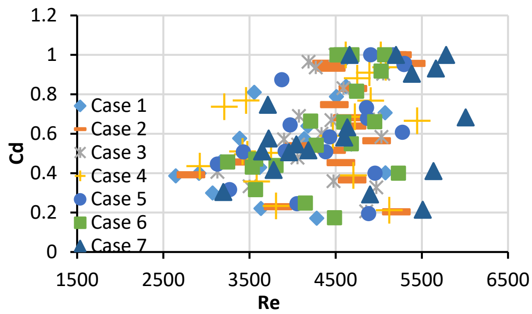

Fig.12 The relation between discharge coefficient and Reynold's number

Figure (13) illustrates the relationship between Reynolds number and $\mathbf{A_g/BH}$. Figure (13) illustrates that the Reynolds number values decrease with an increase in $\mathbf{A_g/BH}$ regardless of the length of obstacle and ccrossssectional aareaofof oobstacleslthealateraldirection. Herthe e, Reynolds number depends on flow depth and flow velocity while $\mathbf{A_g/BH}$ depends on flow depth at upstream. The conflicting hydraulic variables that dominate the Reynolds number and $\mathbf{A_g/BH}$ reflect on their relationship. Figure (14) illustrates the relationship between the discharge coefficient and $\mathbf{A_g/BH}$. Figure (14) illustrates that the discharge coefficient values decrease with an increase in $\mathbf{A_g/BH}$. Here, the obstacle length and cross-sectional area of the obstacle in the lateral direction have major effects on the discharge coefficient values and $\mathbf{A_g/BH}$values. In addition, the inversely proportional relationship between discharge coefficient and $\mathbf{A_g/BH}$will reflect on the relationship between the discharge coefficient and $\mathbf{A_g/BH}$.

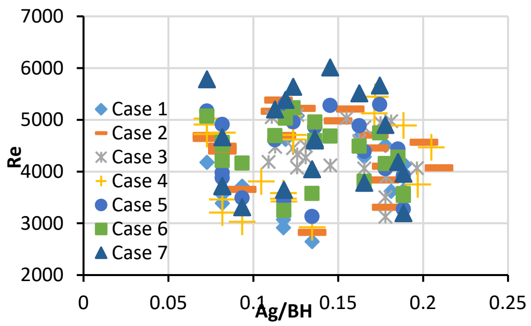

Fig.13 The relation between Reynold's and A_g/BH

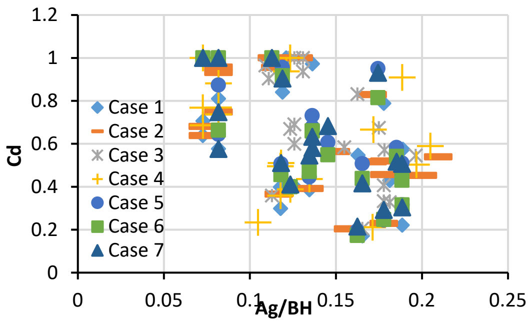

Fig.14 The relation between discharge coefficient and A_g/BH

Figure (15) illustrates the relationship between the actual discharge and A_g/BH. Figure (15) illustrates that the actual discharge values decrease with an increase in A_g/BH. Based on the continuity equation, the actual discharge has a direct proportionality with the flow cross-sectional area that passes the gate. So any increase in flow area will reflect on the actual discharge, but the presence of an obstacle will confine and resist the flow area from the gate and this will reflect on the actual discharge. The relationship between the specific head and the average water depth downstream is shown in figure (16). It is evident from the figure that as the water depth increases, the specific head will increase regardless of the presence of the longitudinal obstacle. The specific head is based on the depth of the water. Furthermore, the relationship between the specific head and the flow velocity downstream is shown in figure (17). It is evident from the figure that as the flow velocity increases, the specific head should be increased regardless of the presence of the longitudinal obstacle.

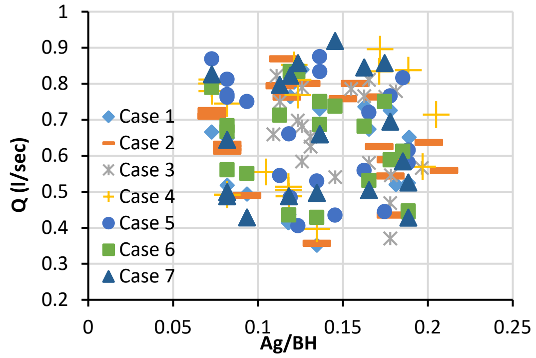

Fig.15 The relation between the actual discharge andA_g/BH

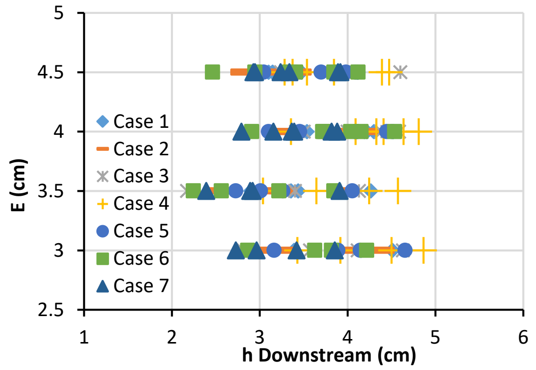

Fig.16 The relation between the specific head and average downstream water depth

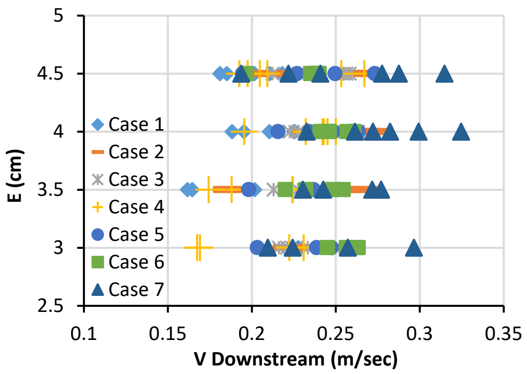

Fig.17 The relation between the specific head and average downstream water velocity

Table (2) comprises a comparison study dealing with weir shape with various obstacles' cross-section dimensions and length. The purpose of this comparison is to reveal the impact of weir shape and obstacles on the average downstream water depth. It is clear from this Table that both maximum and minimum values are more sensitive to the weir

shape, obstacle cross-section, obstacle length, and the interaction between weir flow velocity and gate flow velocity. In general, the previous variables will be prevalent and produce variation in the obtained results. For rectangular weirs, the values of average water depth change from a large value at the obstacle (3cm x 3cm) to a small value at the obstacle (3cm x 1.5cm) and return to the large value at the obstacle (1.5cm x 1.5cm). As well, the values of average downstream water depth for parabola weir and triangular weir are not identical to the values of the rectangular weir. So, we can infer that the longitudinal obstacle produces a random average downstream water depth. For the case without longitudinal obstruction, the maximum and minimum values can be considered moderate values, and these values are more affected by the interaction between weir flow velocity and gate flow velocity.
Table (3) comprises a comparison study dealing with weir shape with various obstacles' cross-section dimensions and length. The purpose of this comparison is to reveal the impact of weir shape and obstruction on the actual discharge. It is clear from Table (3) that both maximum and minimum values are more sensitive to the weir shape, obstacle cross-section, obstacle length, and especially the interaction between weir flow velocity and gate flow velocity. The previous variables will dominate and lead to the variation in the obtained results. This is commonly known as when the cross-section of the obstacle increases, the flow confinement will increase and this will lead to a decrease in the quantity of discharge. Also, when the length of the obstacle increases, the friction losses between the wetted perimeter and flow will increase and lead to a decrease in flow velocity, which leads to a decrease in the quantity of discharge. All the previous reasons are noticeable and prevalent in the obtained values. The fluctuation in results will be attributed to the interference between the discharge from the weir and the gate. It is apparent there is a slight variation in discharge quantity regardless of the existence of the longitudinal obstacle. For the case without a longitudinal obstacle, the maximum and minimum values can be considered comparable values with the cases that adopt the existence of the longitudinal obstacle, and these values are more affected by the interaction between weir discharge and gate discharge.

It was noted from the previous results in Tables (2) and (3) that the maximum and minimum values of downstream water depth and actual discharge in the case of using a longitudinal obstacle are sometimes higher or lower than the maximum and minimum values in the absence of the longitudinal obstacle. Therefore, it appears here the importance of using the statistical hypotheses related to the parameters of the population to decide the value of the mean of the downstream water depth and actual discharge in the case of the use and absence of the longitudinal obstacle. Table (4) shows the mean and standard deviation for the presence and absence of the longitudinal obstacle and the two variables, i.e, the downstream water depth and the actual discharge.

The mean tests were chosen to decide whether to increase or decrease the downstream water depth and the actual discharge as a result of using the longitudinal obstacle. The mean $\boldsymbol{\bar{X}}$ is normally distributed with a mean $\mu = \boldsymbol{\mu_o}$ and standard deviation $\boldsymbol{\sigma_{\bar{x}}}$, so the standard test function variable is normally distributed as follows [13]:

$$\mathbf{Z} = \frac{\bar{\mathbf{X}}-\boldsymbol{\mu}_\mathbf{o}}{\frac{\boldsymbol{\sigma}}{\sqrt{\mathbf{n}}}} \tag{26}$$

The null hypothesis is Ho: $\mu = \boldsymbol{\mu_o}$, while the alternating hypothesis of the higher limit is H1: $\mu > \boldsymbol{\mu_o}$ or of the lower limit is H1: $\mu < \boldsymbol{\mu_o}$ depending on the test condition. The significance level ($\propto = \mathbf{0.01}$) was chosen, noting the number of data used (n= 120).
To test the rate of rising in the downstream water level, the null hypothesis is Ho: $\mu = \boldsymbol{\mu_o}$, there is no rise in the water level at the downstream, while the alternating hypothesis is H1: $\mu > \boldsymbol{\mu_o}$, there is a rise in the water level at downstream as a result of using a longitudinal obstacle. Therefore, the test is one-sided (the right) and the test function is calculated from equation (26) and the test result is (Z = 9.92,) and since the test result is greater than the critical value ($\boldsymbol{Z_{\propto=0.01}} = \mathbf{1.645}$), Ho is rejected and H1 is accepted with high significance. This means that placing longitudinal obstacles at the downstream ends of a composite structure raises the water level.
Similarly, to investigate the effect of the longitudinal obstacles on the actual discharge, the null hypothesis is Ho: $\mu = \boldsymbol{\mu_o}$, that is, there is no difference in the actual discharge for the use or absence of longitudinal obstacles, while the alternating hypothesis is H1: $\mu < \boldsymbol{\mu_o}$, that is, the longitudinal obstacle reduces the amount of actual discharge. Therefore, the test is one-sided (the left) and the test function is calculated from equation (26) and the test result is (Z = -0.166), since the test result is greater than the critical value ($\boldsymbol{Z_{\propto=0.01}} = \mathbf{-1.645}$). So, Ho is accepted and H1 is rejected with high significance. That is, placing the longitudinal obstacles does not underestimate the actual discharge.

Table 2 The minimum and maximum value of average downstream water depth for different weir shapes and obstacle dimensions

Weir Shape	X-section	average(cm)					
		Length=90cm		Length=60cm		Length=0cm	
		Min.	Max.	Min.	Max.	Min.	Max.
Rectangle	3cm*3cm	3.1	4.5	3.3	4.6		
	3cm*1.5cm	2.8	4.3	3.3	4.4		
	1.5cm*1.5cm	3.2	4.3	2.9	4.5		
	0*0					2.9	3.9
Parabola	3cm*3cm	3.1	4.3	3.2	4.8		
	3cm*1.5cm	3.2	4.3	3.0	4.5		
	1.5cm*1.5cm	2.9	4.6	2.5	4.1		
	0*0					2.7	3.9
Triangle	3cm*3cm	2.9	4.5	3.0	4.8		
	3cm*1.5cm	2.5	4.3	2.7	4.6		
	1.5cm*1.5cm	2.2	4.6	2.2	4.2		
	0*0					2.4	3.9

Table 3 The minimum and maximum value of Actual Discharge for different weir shapes and obstacle dimensions

Weir Shape	X-section	$Q_{act.}$(l/s)					
		Length=90cm		Length=60cm		Length=0cm	
		Min.	Max.	Min.	Max.	Min.	Max.
Rectangle	3cm*3cm	0.436	0.764	0.487	0.895		
	3cm*1.5cm	0.434	0.868	0.483	0.868		
	1.5cm*1.5cm	0.545	0.822	0.435	0.833		
	0*0					0.487	0.918
Parabola	3cm*3cm	0.420	0.725	0.503	0.837		
	3cm*1.5cm	0.543	0.800	0.444	0.874		
	1.5cm*1.5cm	0.468	0.810	0.443	0.868		
	0*0					0.427	0.875
Triangle	3cm*3cm	0.351	0.838	0.396	0.810		
	3cm*1.5cm	0.356	0.793	0.405	0.833		
	1.5cm*1.5cm	0.370	0.681	0.428	0.833		
	0*0					0.428	0.796

Table 4 Statistic Parameter of State variables

Variable	$h_{daverage}$ (cm)		$Q_{act.}$ (l/sec)	
	Mean	Standard Deviation	Mean	Standard Deviation
Without Obstacle ($\boldsymbol{\mu_o}$,σ)	3.28	0.46	0.651	0.165
With Obstacle ($\boldsymbol{\mu}$, $\boldsymbol{\sigma_{\bar{x}}}$)	3.71		0.648	

6. CONCLUSION

The following should be noted from the current paper:

1- The longitudinal obstacle has a moderate effect on the hydraulic characteristics of the composite hydraulic structure.
2- The hydraulic response of the composite hydraulic structure for cases from the case (1) to case (6) is similar to the hydraulic behavior of the composite hydraulic structure in case (7).
3- The length of the obstacle has a minor effect as compared with its lateral dimensions.
4- The interference between the weir flow velocity and the gate flow velocity has important effects on the fluctuation of the obtained results.
5- The interaction between various hydraulic variables and the presence of the obstacle will control the response of the composite hydraulic structure.

6- The water depth and water velocity in the downstream region are more affected by the obstacle.
7- Good results are obtained for the estimated values of the head regardless of the obstacle presence.
8- The actual discharge and the flow which passes the gate are more sensitive to the presence of the obstacle.
9- Due to the important role of the flow which passes the gate in the assessment of the hydraulic response of the composite hydraulic structure, this research concentrated on the relationship between the ratio $\boldsymbol{A_g/BH}$ and actual discharge, discharge coefficient, Froude number, and Reynolds number.
10- A hypothesis test on the downstream water level and actual discharge are performed. The results give evidence that using longitudinal obstacles downstream of a composite structure raises the water level and does not underestimate the actual discharge.

7. REFERENCES

[1] Qasim, R. M., Abdulhussein, I. A., and Al-Asadi, K., The Effect of Barrier on the Hydraulic Response of Composite Weir-Gate Structure, Archives of Civil Engineering, Vol. 4, Issue LXVI, 2020.

[2] Qasim, R. M., Abdulhussein, I. A., Mohammed, A.A. and Maatooq, Q. A., The Effect of the Obstacle on the Hydraulic Response of the Composite Hydraulic Structure, Incas Bulletin, Vol. **12**, No.3, 2020, p. 159 – 172.

[3] Riazi, R. and Jafari, S., The Characteristics of Submerged Hydraulic Jump in Sloped Stilling Basins with Rough Bed, Bulletin of Environment. Pharmacology and Life Sciences, Vol. **3**, No. 6, 2014, p. 238-243.

[4] Samadi-Boroujeni, H., Ghazali, M., Gorbani, B. and Fattahi Nafchi, R., Characteristics of Hydraulic Jump on Corrugated Beds, Canadian Journal of Civil Engineering, Vol. **40**, No. 9, 2013, p. 841-847.

[5] Nabil, B. and Rezak, A. A., Effect of Baffle Blocks with Sloping Front Face on the Length of the Jump, Journal of civil engineering institute of engineers, Bangladesh, Vol. **30**, No. 2, 2002, p. 101-108.

[6] Hughes, W. C., and Flack, J. E., Hydraulic Jump Properties Over a Rough Bed, J. Hyd. Div., ASCE, Vol. **110**, 1984, p. 1755-1771.

[7] Mohamed Ali, H. S., Effect of Roughened-Bed Stilling Basin on Length of Rectangular Hydraulic Jump, J. Hydraulic Eng., ASCE, Vol. **117**, No. 1, 1991, p. 83-93.

[8] Streeter, V. L., and Wylie, E. B., Fluid Mechanics, First SI Metric Edition, 1983.

[9] Bos, M. G., Discharge Measurement Structures, 3rd Edition International Institute for Land Reclamation and Improvement/ Wageningen, The Netherlands, 1989.

[10] Chow, V. T., Open-Channel Hydraulics. McGraw-Hill, 1983.

[11] Fox, R. W., and McDonald, A. T., Introduction to Fluid Mechanics, Fourth Edition, SI version Copyright © John Wiley and Sons, Inc., 1994

[12] Munson, B. R., Young, F. D., Okishi, H. T. and Hubsch, W. W., Fundamentals of Fluid Mechanics. Sixth edition, John Wiley & Sons, Inc., 2009.

[13] Vining, G. and Kowalski, S. M., Statistical Methods for Engineers, Third Edition, CENGAGE Learning, 2011.